IEEE Access
Multidisciplinary ⋮ Rapid Review ⋮ Open Access Journal

Received May 19, 2021, accepted June 22, 2021, date of publication June 25, 2021, date of current version July 5, 2021.

Digital Object Identifier 10.1109/ACCESS.2021.3092558

Feedforward for Robust Reference Tracking in Multi-Input Feedback Control

JAVIER RICO-AZAGRA AND MONTSERRAT GIL-MARTÍNEZ
Control Engineering Research Group, University of La Rioja, 26004 Logroño, Spain
Corresponding author: Javier Rico-Azagra (javier.rico@unirioja.es)

This work was supported by the University of La Rioja under Grant REGI 2020/23.

This work did not involve human subjects or animals in its research.

ABSTRACT This paper examines methods to incorporate feedforward loops of known external inputs (output reference) into a multi-input feedback control structure to achieve certain robust performance of its output. Undoubtedly, feedforward can reduce the need for feedback and therefore the amplification of sensor noise at actuators, as occurs in single-input control. Beyond that, since there are several available inputs, a convenient distribution of feedforward and feedback can minimise the control action at each input and offer benefits at all frequencies. The procedure is as follows: because there are rough plant models of the behaviour from each input to the output, it is possible to approximate the individual control demand that will satisfy the performance. Based on this, individual feedforward filters allocate the control bandwidth among the inputs in order to build an equivalent plant that has an equal or greater magnitude than any individual plant at each frequency. Next, the uncertainty of this equivalent plant is addressed by feedback that reduces the closed loop deviation of magnitude frequency responses. The reduction is sufficient to enable a master feedforward to place them, at a second step, around the desired tracking performance model without violating any deviation tolerances. Individual feedback controllers distribute the total feedback among the inputs in order to have the least possible feedback at each frequency. A first example illustrates the method and the relevance of a feedforward orientation to reduce the individual control action, instead of the individual feedback action. Another example proves the superiority of adding feedforward loops to feedback-only schemes and highlights the benefits of robust design methods such as Quantitative Feedback Theory (QFT). This paper also provides the algorithms to employ in response to new robust control specifications in the framework of QFT.

INDEX TERMS Mid-ranging control, valve position control, control allocation, robust control, quantitative feedback theory, model-matching, tracking error.

I. INTRODUCTION

In some cases, several inputs are available to govern the output of feedback control, which is described here as a multiple-input single-output (MISO) control. Successful examples of the latter can be found in many different disciplines. They include process control [1]–[3], medical systems [4], consumer electronics [5], [6], robotics [7]–[9], unmanned aerial vehicles [10], and the automotive industry [11].

In single-input single-output (SISO) control, the limited capacity of the single actuator limits the performance that can be achieved at the output. Or, if the performance is prioritized, this determines the necessary control action. However, several combinations of the manipulated inputs can contribute to the required output performance in MISO control. Various structures and methodologies to accomplish this appear in the scientific literature. One area of work focuses on hierarchy structures [12]. A high-level controller produces the virtual (total) control action that is necessary to achieve the output performance. Then, a low-level *control allocation* algorithm coordinates the set of multiple inputs to produce the virtual control action. Selecting the best of the feasible inputs at each time is at the heart of different approaches. Some of these solve optimization problems [13] addressing different criteria such as input constraints, consumption and output performance. There is another area of work branded

The associate editor coordinating the review of this manuscript and approving it for publication was Rongni Yang.

as *valve position control* [14] and *habituating control* [15]. In these methods, two inputs participate along different frequency bands. Thus, the cheapest and most powerful input dominates the steady state, while the most expensive and fastest input provides the dynamic performance and returns to a convenient resetting point in the steady state. *Mid-range* resetting points attempt to preserve the maximum actuation range in the event that a new output deviation occurs [16]. Any other resetting points might inspire the establishment of a more profitable steady state of the manipulated inputs [2], [17]. One paper [18] presents a general setting of n inputs whose sequential intervention can be selected as desired. A robust design of feedback controllers achieves this in the framework of Quantitative Feedback Theory (QFT).

The criteria for assigning a frequency band to each control input can be linked to the input itself; this includes its range and associated cost, the sensor noise amplification at the control input, or the static and dynamic constraints of the actuator. Furthermore, those criteria may depend on the contribution of the control input to the output, i.e. the plant frequency response, and its constraints. Inputs (plants) that do not produce any significant benefit are not called to collaborate at a specific frequency for two main reasons. First, an unnecessary contribution of one input in the steady state displaces its equilibrium point which reduces the actuation range of its dynamic contribution. Second, an unfruitful contribution of one input in non-zero frequencies unnecessarily excites the actuators. Therefore, it is important to determine how to make the most of the frequency response of each individual input (plant) in order to save individual control effort while achieving the performance. In a MISO structure with only feedback control elements, this is equivalent to designing the set of feedback controllers that have the lowest possible gain at each frequency. Quantitative and robust solutions to this were provided in [19], [20]. Further insights are required when feedforward elements participate in robust control tasks together with feedback controllers, to which the present work will contribute.

Feedforward conveniently channels the information from known external inputs (output reference or measurable disturbances) which, in SISO control, enables a reduction in the amount of feedback (=feedback controller gain), and then softens the mid-high frequency drawbacks of feedback (sensor noise amplification at the control input). QFT seeks to reducing the amount of feedback to what is strictly necessary for the existence of a feedforward element [21], [22]. The feedforward mainly provides the desired output behaviour for the external input change, whereas the feedback constrains the closed-loop dispersion due to plant model uncertainty. Nevertheless, whatever the roles of feedback and feedforward, the total control action would be invariable. This is because the required output performance can be contributed by a single input (plant). This does not happen in multi-input systems where, eventually, sensible distribution of feedback and feedforward can reduce the control effort at each actuation, as the present work will demonstrate. New control architectures will permit a tailor-made and separated contribution of feedback and feedforward for each control input. Then, the matter of how to share the frequency band among inputs for feedback and feedforward will be studied. Uncertainty in plant models will be explicitly considered. The QFT framework will provide the methodology for the design of the control elements that achieve the required robust stability and reference tracking performance while reducing the individual control effort. New quadratic inequalities to compute QFT bounds will be required to make decisions and to design the control elements.

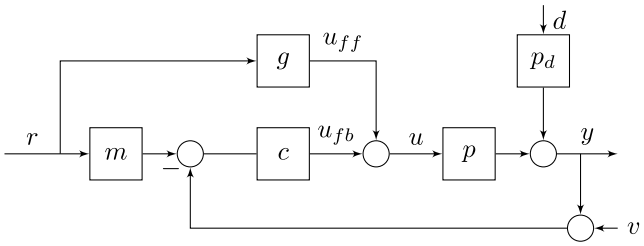

FIGURE 1. Feedback-feedforward control structure for SISO control [22].

The remaining paper is organized as follows: Section 2 includes the new control architecture and the design method. Section 3 presents two examples: the first shows a well-performed distribution of feedback and feedforward and the second shows the superiority of adding feedforward to classical feedback structures. Section 5 gives the conclusions. An Appendix provides the formulation for QFT designs.

II. ROBUST REFERENCE TRACKING

A. PRELIMINARIES: THE SISO CASE

Let us take the feedback-feedforward control structure in Fig 1 (model-matching [22]), as the most convenient example: (i) to discern the roles of feedback $c(s)$ and feedforward $g(s)$, (ii) to relate them to the required y/r performance by the explicit model m, and (iii) to obtain both actions, u_{fb} and u_{ff}, separately.

Feedforward could achieve perfect control in r reference tracking ($m-y/r=0$) with $g=m/p$ under the ideal assumption that there is no modelling error in plant p. The lack of reality of this (together with the presence of unknown d disturbances) justifies the feedback correction with c, which introduces sensor noise v as a negative counterpart. The tracking error is

$$e=\frac{m-p\,g}{1+p\,c}r-\frac{1}{1+p\,c}v-\frac{p_d}{1+p\,c}d \tag{1}$$

and the control action can be written as

$$u=\left(\frac{m-p\,g}{1+p\,c}c+g\right)r-\frac{c}{1+p\,c}v-\frac{c\,p_d}{1+p\,c}d. \tag{2}$$

The two terms for the function u/r split feedback and feedforward actions, u_{fb} and u_{ff}, with respect to r.

Robust reference tracking considers explicit uncertainty in the model p to design c and g. In particular, the *model-matching* version [22] of QFT limits every possible y/r in

the ω frequency domain so that

$$\left|m-\frac{y}{r}\right| = \left|\frac{e}{r}\right| = \left|\frac{m-p\ g}{1+p\ c}\right| \leq W_r; \quad \forall p,\ \forall \omega, \tag{3}$$

where W_r is a magnitude tolerance on closed-loop deviations of y/r around the desired tracking model m. The robust specification (3) can be fulfilled only with the feedback element c, and the feedfoward element $g = 0$. However, it is obvious that g can conveniently reduce $|m - p\ g|$ and consequently, less feedback c is needed. Eventually, this reduces the *cost of feedback* [21], i.e. the v noise amplification at the u actuator (2). Accordingly, one study [22] develops the formulation to cause the design of g and c to be independent so that the feedback demand c is limited to what is strictly necessary for a feedforward controller g. Thus, feedback c reduces the dispersion of the set of frequency responses y/r to what a feedforward g can position around m and meet (3). This implies a control effort u/r (2) whose magnitude frequency response can be broken down in feedback u_{fb}/r and feedforward u_{ff}/r terms that can be over-bounded as follows

$$\begin{aligned}\left|\frac{u}{r}\right| &= \left|\frac{u_{fb}}{r}+\frac{u_{ff}}{r}\right| \\ &= \left|\frac{m-p\ g}{1+p\ c}c+g\right| \leq W_r|c|+|g|; \quad \forall p,\ \forall \omega. \end{aligned} \tag{4}$$

At a first glance, $W_r|c|$ takes relative small values along the frequency, since the tracking tolerance W_r is small along the control bandwidth and the feedback demand $|c|$ reduces beyond the cross over frequency. Let us roughly approximate $g = m/p_o$, assuming that p_o is the middle plant in the uncertain set of p plant frequency responses. Then, $|m/p_o|$ usually results in far greater than $W_r|c|$, unless there was great plant uncertainty that would magnify $|c|$ or unless there were large plant magnitudes that would shrink $|g|$. All this means feedforward action is usually greater than feedback action. Furthermore, the absence of feedforward g should be supplied by feedback c. In such a case, a rough upper tolerance of the u_{fb}/r magnitude frequency response could be $(|m| + W_r)/|p_{\min}|$ (assuming that $p_{\min}$ is the plant of least magnitude in the set p). In summary, the magnitude of the plant set roughly configures the control demand at each frequency, regardless of whether it is provided only with feedback or with feedforward assistance.

Then, if several plants (inputs) were available to provide the performance (m, W_r), those plants of greatest magnitude would demand less control action. Furthermore, if feedback and feedforward build the control action, it is usually the feedforward action that is greatest in magnitude. With these preliminaries, the aim is to allocate the frequency band among the available inputs after studying each output-input (plant) frequency response.

B. MISO CONTROL

A new feedback-feedforward control structure is adapted to MISO systems for reference tracking in Fig 2. The y output deviation is modelled by the influence of $u_{i=1,\dots n}$ manipulated inputs and a non-measurable d disturbance input. Thus, a vector of $(n + 1)$ transfer functions, $P(s) = [p_{i=1,\dots n}(s), p_d(s)]$, defines the MISO plant. Let us assume a total amount of w uncertain parameters in these dynamical models. By defining q_l as a vector of those uncertain parameters in the set of the all the possible values $\mathcal{Q}$ in $\mathbb{R}^w$, the MISO uncertain plant can be formally defined as

$$\mathcal{P} = \{P(s; q_l) : q_l \in \mathcal{Q}\}. \tag{5}$$

Henceforth, labels p_i (or p_d) denote plants with uncertainty, which can adopt any model in the set (5).

Individual control elements c_i and g_i allow an independent distribution of feedback and feedforward tasks, respectively, for each control action u_i, which commands a plant p_i. As a result, the total feedback

$$l_t = \sum_{i=1}^{n} l_i = \sum_{i=1}^{n} p_i c_i \tag{6}$$

is contributed by individual feedback loops l_i. And the total feedforward

$$l_g = \sum_{i=1}^{n} l_{g_i} = \sum_{i=1}^{n} p_i g_i\ g_m \tag{7}$$

is contributed by individual feedforward channels l_{gi}.

The matching of the frequency responses y/r to the desired behaviour m is confined in magnitude such that

$$\begin{aligned}\left|m-\frac{y}{r}\right| &= \left|\frac{e}{r}\right| = \left|\frac{m-l_g}{1+l_t}\right| \\ &= \left|\frac{m-\sum_{i=1}^{n} p_i g_i g_m}{1+\sum_{i=1}^{n} p_i c_i}\right| \leq W_r; \quad \forall P \in \mathcal{P},\ \forall \omega. \end{aligned} \tag{8}$$

As a main difference with SISO control (3)(4), several combinations of $u_{i=1,\dots,n}/r$ can now achieve (8). Depending on the role that is attributed to feedback and feedforward for each input, u_i/r can be broken down in feedback and feedforward terms, and its magnitude frequency response can be over-bounded as

$$\begin{aligned}\left|\frac{u_i}{r}\right| &= \left|\frac{u_{fb_i}}{r}+\frac{u_{ff_i}}{r}\right| = \left|\frac{m-\sum_{i=1}^{n} p_i g_i g_m}{1+\sum_{i=1}^{n} p_i c_i}c_i + g_i g_m\right| \\ &\leq W_r|c_i| + |g_i g_m|; \forall P \in \mathcal{P},\ \forall \omega. \end{aligned} \tag{9}$$

The final objective is to meet the robust tracking specification (8) while using the least possible control action at each input $|u_i/r|$. With this aim, the feedforward distribution by g_i is addressed first, and then, the feedback by c_i. The master g_m completes the fulfilment of specification. A frequency domain method will be followed. Depending on the gain associated with g_i and c_i at ω, the plant p_i will contribute to achieving or not achieving the specification at ω.

C. FEEDFORWARD DISTRIBUTION AMONG INPUTS

This first stage studies and executes the feedforward distribution. Feedforward elements $g_{i=1,\dots,n}(j\omega)$ are filters with

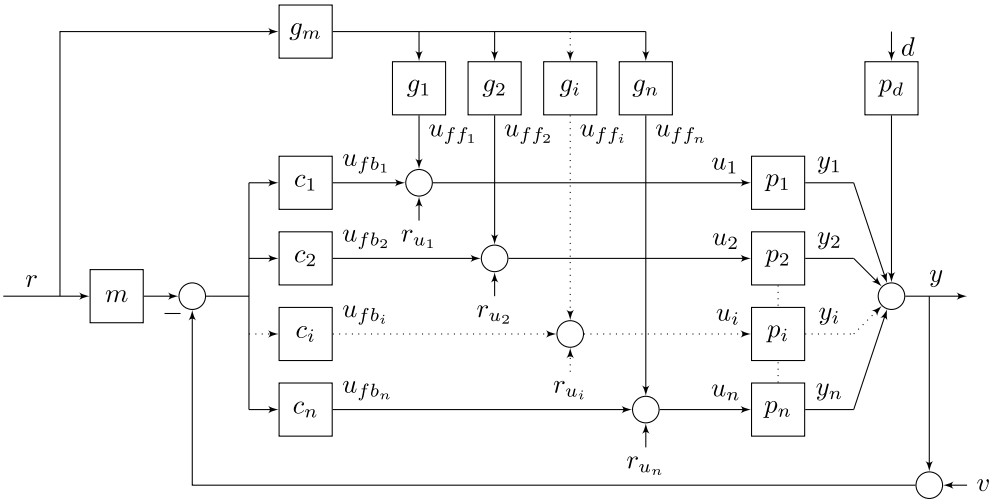

FIGURE 2. Feedback-feedforward control structure for robust reference tracking in multi-input systems.

unitary gain at the frequencies where the p_i participation is of interest. This yields the plant

$$p_m = \sum_{i=1}^{n} p_i g_i, \tag{10}$$

whose uncertainty will be conveniently reduced by total feedback l_t and then positioned by g_m (8) in later stages of design.

At a first glance, the strategy is to get the smallest uncertainty of p_m at each frequency,

$$\min\left(\left|m - l_g\right|\right); \quad \forall P \in \mathcal{P},\ \forall \omega, \tag{11}$$

which foretells smaller feedback l_t and therefore smaller controller gains $|c_i|$. This would reduce the sensor noise amplification at each input, since $|u_i/v|$ is reduced. Magnitudes $|u_{fb_i}/r|$ would also be reduced (9). However, this could occur at the expense of a large increase of $|u_{ff_i}/r|$ due to $|g_m|$ growth. That would be the case if p_m does not have the maximum achievable gain. Section II-A concluded that plant magnitude mainly conditions the control action.

Therefore, the best strategy is to get the highest gain of p_m (10) at each frequency, which implies a feedforward routing by g_i to the most powerful p_i plants regardless of their uncertainty. With this goal, it is proposed to begin by computing an approximation of the frequency response function u_i/r, in the event that only input u_i will provide the performance m,

$$k_i = \frac{m}{p_{i,\min}}; \quad \forall P \in \mathcal{P},\ \forall \omega \tag{12}$$

where $p_{i,\min}$ is the plant p_i of least magnitude at a particular ω inside the uncertain set $|p_i(j\omega)|$. Next, the k_i frequency responses of all inputs $i = 1, \ldots, n$ are compared at each frequency to decide which inputs are of sufficient interest for participation: those that yield the smallest k_i magnitude are considered. At any frequency, the contribution of as many inputs as possible is desired, if it yields a total plant p_m (10) with *significantly* greater magnitude than the individuals p_i (let us remember that g_i are filters with unitary gain at the pass band). Thus, their potential collaboration would reduce the individual feedforward actuations $|u_{ff_i}/r|$ because of the virtual need for total feedforward $|u_{ff}/r| \approx |m/p_m|$ would be significantly reduced. A two-in-two comparison of k_i is advised. As a rule of thumb, a difference in $k_i(j\omega)$ magnitude greater than $20\log 2 = 6$ dB makes the plant that is associated to larger $k_i(j\omega)$ magnitude useless. A second relevant point is to check that the $k_i(j\omega)$ phase-shift of those plants that are likely to collaborate is less than 90°, since the vector sum of plants in counter-phase would reduce the total magnitude of p_m (10).

After the comparisons, the feedforward frequency band is distributed among the inputs, which can work in separated bands or collaborate within the same band. Finally, to attain the planned distribution, the g_i filters have an open-loop design. As a result, the magnitude of $p_m(j\omega)$ in (10) should be equal to or exceed than the magnitude of any $p_i(j\omega)$.

Once the g_i filters are known, the remaining specification (8) becomes

$$\left|\frac{e}{r}\right| = \left|\frac{m - p_m g_m}{1 + \sum_{i=1}^{n} p_i c_i}\right| \leq W_r; \quad \forall P \in \mathcal{P},\ \forall \omega. \tag{13}$$

Next, the $c_{i=1,\ldots,n}$ feedback task is reducing the closed-loop influence of the p_m uncertainty to the extent that a master feedforward g_m can position the resulting y/r frequency responses around m with a magnitude deviation less than W_r tolerance.

D. FEEDBACK DISTRIBUTION AMONG INPUTS

The total feedback needed, $l_t = \sum_{i=1}^{n} p_i c_i$, can be provided by several inputs (or p_i plants). In particular, this stage first examines how to distribute the feedback frequency band among the inputs. The design of $c_{i=1,\ldots,n}(j\omega)$ is accomplished in a second step. The purpose is to use the least possible amount of feedback (controller gain) at each frequency, since this results in saving the individual feedback control action $|u_{fb_i}/r|$ in (9). Thus, it is proposed to compare the *exact* amount of feedback $|c_i(j\omega)|$ that each p_i plant would require to achieve the specification by itself ($c_{k\neq i} = 0$).

If only p_i participates in feedback tasks, (13) becomes

$$\left|\frac{m - p_m g_m}{1 + p_i c_i}\right| \leq W_r; \quad \forall P \in \mathcal{P},\ \forall \omega. \tag{14}$$

Despite its similarity with (3), p_m and p_i are different plants and it is not possible to use the QFT formulation [22] to make the design of feedback c_i independent of feedforward g_m. A new formulation is developed in Appendix IV. This also provides the quadratic inequalities to incorporate in the Terasoft QFT toolbox [23] in order to compute the bounds that guide the design of c_i.

Appendix IV deals with control specifications that follow the general format

$$\left|\frac{AG_f + B}{C + DG}\right| \leq W. \tag{15}$$

In comparing (14) and (15), let us take $A = -p_m$, $B = m$, $C = 1$, $D = p_i$, $G = c_i$, $G_f = g_m$ and $W = W_r$, to compute the QFT bounds $\beta_{l_i}(\omega)$ for a discrete set Ω of ω-frequencies. Depicted on mod-arg plots, the bounds express the closed-loop restriction (14) in terms of a nominal open-loop transfer function $l_{i_o} = p_{i_o} c_i$ where p_{i_o} is any plant in the uncertain set p_i that is chosen as the nominal plant.

The exact amount of feedback $|c_i(j\omega)|$ at each design phase can be computed by $\beta_{c_i}(\omega) = \beta_{l_i}(\omega)/|p_{i_o}(j\omega)|$. Then, bounds $\beta_{c_i}(\omega)$ are computed for all inputs $i = 1, \ldots, n$. Once they are depicted on mod-arg plots, their magnitude heights and their phase-shifts are compared at each discrete $\omega \in \Omega$. In essence, β_{c_i} bounds of lower magnitude height imply less $|c_i|$ if p_i plant were employed and, then, less $|u_{fb_i}/r|$ (9). Furthermore, the contribution of as many inputs as possible is desirable at each frequency whenever their contribution would imply a significant reduction of $|u_{fb_i}/r|$. A rule of thumb is to choose the inputs of lower β_{c_i} magnitude height with a difference that does not exceed $20\log q$ dB (q is the number of plants asked to collaborate). In this way, since l_t is the total feedback to obtain, the contribution of q plants of similar magnitude $|p_i(j\omega)|$, that is $l_t = \sum_{i=1}^{q} l_i$, would reduce the need $|c_i(j\omega)|$ (and then, $|u_{fb_i}/r|$) by approximately q times. It should be noted that if only one plant works ($q = 1$), then $l_t = l_i$. Another relevant point is determine if the β_{c_i} phase-shift of plants that are likely to collaborate is less than 90°. It should be recalled that loops in counter-phase would impair the increase in magnitude to reduce the control action. After completing these magnitude and phase comparisons, the feedback frequency band is distributed among the inputs, which can work in separated bands or collaborate in the same band.

Finally, to attain the planned distribution, the set of controllers c_i are designed via the loopshaping of $l_i(j\omega)$ to satisfy the bounds $\beta_{l_i}(\omega)$ at Ω, following a sequential process between the i loops. Thus, if at some point, the controller c_i is to be adjusted and the other controllers $c_{k\neq i}$ take known values in the sequence, the robust tracking specification (13) can be rewritten as

$$\left|\frac{m - p_m g_m}{1 + \sum_{k\neq i} p_k c_k + p_i c_i}\right| \leq W_r(\omega); \quad \forall P \in \mathcal{P},\ \forall \omega. \tag{16}$$

and their representative β_{l_i} bounds can be computed by choosing $A = -p_m$, $B = m$, $C = 1 + \sum_{k\neq i} p_k c_k$, $D = p_i$, $G = c_i$, $G_f = g_m$ and $W = W_r$ in the solution given to (15) in the Appendix IV. The loopshaping essence is that c_i provides the necessary gain at the frequencies where p_i plant must work and filters those frequencies where p_i must not work. Special attention must be paid at the frequencies where several inputs must collaborate. A detailed explanation on the global procedure is given in [19].

E. FULFILLING SPECIFICATIONS

Achieving tracking error specification (8) ends with the design of g_m. Since elements g_i and c_i are known, the specification resembles the format $|(A + BG)/(C + DG)| \leq W$ that implements the function *gndbnds* in [23]. By choosing $A = m$, $B = -\sum_{i=1}^{n} p_i g_i$, $C = 1 + \sum_{i=1}^{n} p_i c_i$, $D = 0$, $G = g_m$, and $W = W_r$, the regions for g_m that are permitted are computed. A certain over-design in the gain of $c_{i=1,\ldots n}$ may be desirable to enlarge these regions and simplify the shaping of the feedforward master g_m. Let us remember that this is accomplished on a mod-arg plot, as suggested in [22], [24].

Besides their task in robust reference tracking, feedback controllers must achieve certain robust stability. Constraints on global sensitivity or complementary sensitivity [19] may not be sufficient to assure certain stability margins for any single loop. Then, specifications of the type

$$|T_i| = \left|\frac{l_i}{1 + l_t}\right| \leq W_{s_i}, i = 1, \ldots, n; \quad \forall P \in \mathcal{P},\ \forall \omega, \tag{17}$$

are advised [18], [20], [25], where W_{s_i} delimits the size of the forbidden region around the critical point that cannot be violated by $l_i = c_i p_i/(1 + \sum_{j\neq i} l_j)$. Their representative bounds can be computed with traditional CAD tools in the QFT toolbox [23]. Thus, at each ω-frequency in Ω, a set of n stability bounds and one tracking bound are combined to give a single representative bound. Next, the set of bounds at Ω are met by $l_i(j\omega)$ shaping.

Specifications for the robust rejection of non-measurable d-disturbances are

$$\left|\frac{e}{d}\right| = \left|\frac{p_d}{1 + l_t}\right| \leq W_d; \quad \forall P \in \mathcal{P},\ \forall \omega. \tag{18}$$

Since no feedforward of d is possible, the feedback must do all the work. Choosing the inputs better conditioned to provide both performances (reference tracking and disturbance rejection) can reduce u_{fb_i} due to r and d. Thus, in addition to β_{c_i} bounds for (14), new β_{c_i} bounds must be computed to represent $|p_d/(1 + p_i c_i)| \leq W_d$. In this last case, classical functions in the QFT toolbox [23] can be used to compute the bounds β_{l_i} on l_{i_o}, and then, $\beta_{c_i} = \beta_{l_i}/|p_{i_o}|$.

Some important issues of MISO control from the point of view of its practice application should be noted. Consider how the whole set of external inputs, $r, d, v, r_{u_{i=1,\dots,n}}$ in Fig 2 intervene in the tracking error

$$e = \frac{m - l_g}{1 + l_t} r - \frac{1}{1 + l_t} v - \frac{p_d}{1 + l_t} d - \sum_{i=1}^{n} \frac{p_i}{1 + l_t} r_{u_i}, \quad (19)$$

and in each control action

$$u_i = \left[\frac{m - l_g}{1 + l_t} c_i + g_i g_m \right] r - \frac{c_i}{1 + l_t} (v + p_d d) + \frac{(1 + l_{-i})}{1 + l_t} r_{u_i} - \sum_{k \neq i} \frac{c_i p_k}{1 + l_t} r_{u_k}, \quad (20)$$

where $l_{-i} = l_t - l_i$.

A zero steady state error $e(t = \infty) = 0$ is usually desired. In the frequency domain, this involves $|l_t(j0)| = \infty$, which makes $1 + l_t(j0) \approx l_t(j0)$, and the frequency response of (19) becomes

$$e(j0) \approx \frac{m(j0) - l_g(j0)}{l_t(j0)} r(j0) - \frac{1}{l_t(j0)} v(j0) - \frac{p_d(j0)}{l_t(j0)} d(j0) - \sum_{i=1}^{n} \frac{p_i(j0)}{l_t(j0)} r_{u_i}(j0). \quad (21)$$

To achieve $|l_t(j0)| = \infty$, at least one $l_i(j\omega)$ of the $i = 1, \dots, n$ loops should work at the lowest frequency band ($|l_i(j0)| = \infty$). Thus, the c_i controller should provide the necessary number of integrators to cancel the influence of $r(j0)$, $v(j0)$, $d(j0)$ and $r_{u_i}(j0)$ on $e(j0)$.

Another common requirement is that the control variables that do not work at steady state can return to convenient set points [2], [14]-[18]. Thus, let us impose $u_k(t = \infty) = r_{u_k}(t = \infty)$ in the event that l_k does not work in the steady state. The k control action (20) can be approximated at $\omega = 0$ as

$$u_k(j0) \approx \left[\frac{m(j0) - l_g(j0)}{l_t(j0)} c_k(j0) + g_k(j0) g_m(j0) \right] r(j0) - \frac{c_k(j0)}{l_t(j0)} (v(j0) + p_d(j0) d(j0)) + \frac{l_t(j0) - l_k(j0)}{l_t(j0)} r_{u_k}(j0) - \sum_{i \neq k} \frac{c_k(j0) p_i(j0)}{l_t(j0)} r_{u_i}(j0) \quad (22)$$

where $|l_t(j0)| = \infty$. If c_k contains an inferior number of integrators than the loops that work in the low frequency band, it means that $|l_k(j0)| \ll |l_t(j0)|$ and $|c_k(j0)| \ll |l_t(j0)|$, and (22) becomes

$$u_k(j0) \approx g_k(j0) g_m(j0) r(j0) + r_{u_k}(j0). \quad (23)$$

Thus, to meet $u_k(t = \infty) = r_{u_k}(t = \infty)$ an additional requirement at $\omega = 0$ is $|g_k(j0)| = 0$, i.e. g_k should have the necessary number of differentiators that eliminate the influence of $r(j0)$ on $u_k(j0)$. In summary, the k-branch should not work at low frequencies in feedback or feedforward tasks.

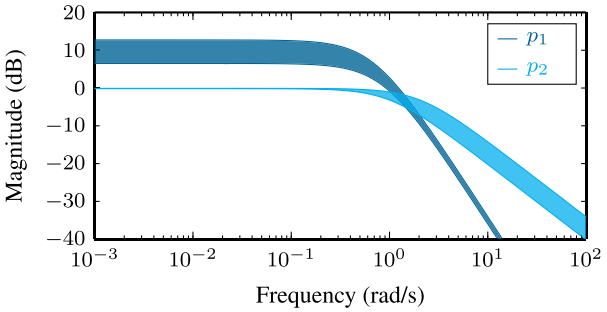

FIGURE 3. Magnitude frequency responses of plants.

III. EXAMPLES

Below, two examples show the new methodology along with some comparisons that illustrate its benefits. A two-input system ($i = 1, 2$) is considered, whose plant models are

$$p_1(s) = \frac{a}{\left(s + \frac{b}{a}\right)^2}, \quad p_2(s) = \frac{c \cdot d}{s + d}$$
$$a \in [1.60,\ 2.00], \quad b \in [1.36,\ 1.44]$$
$$c \in [0.98,\ 0.99], \quad d \in [1,\ 3]. \quad (24)$$

Fig 3 shows that $p_1(j\omega)$ is more powerful, but with a greater uncertainty than $p_2(j\omega)$ in low frequencies. The opposite occurs in high frequencies.

A. EXAMPLE 1

This first example illustrates how a convenient distribution of feedback and feedforward among the available plants (24) can reduce the control action at each input. The main control goals are to achieve robust stability and robust reference tracking performance. Robust stability specifications (17) seek minimum phase margins (PM) of 40° by taking

$$W_{s_{i=1,2}} = \left| \frac{0.5}{\cos(\pi(180 - PM)/360)} \right|, \quad PM = 40°. \quad (25)$$

Robust model-matching in reference tracking (8) takes the form

$$m(s) = \frac{32.65}{s^2 + 8s + 32.65}, \quad (26)$$

and the deviation tolerance

$$W_r(\omega) = \left| \frac{0.2s}{0.125s^2 + 0.75s + 1} \right|_{s=j\omega}. \quad (27)$$

The set of discrete frequencies is

$$\Omega = \{0.01,\ 0.1,\ 0.2,\ 0.4,\ 0.8,\ 1,\ 4,\ 8,\ 10,\ 20\}[\text{rad/s}]. \quad (28)$$

Two strategies are compared for feedforward distribution. The former (ST1) attempts to reduce the individual control action by considering $k_i(j\omega)$ (12) as indicated in Section II-C. k_i frequency responses are depicted in Fig 4, concluding the allocation at the upper part of Table 1. A second strategy (ST2) aims for (11), which rewards those p_i plants with less uncertainty (see Fig 3) to reduce the individual feedback

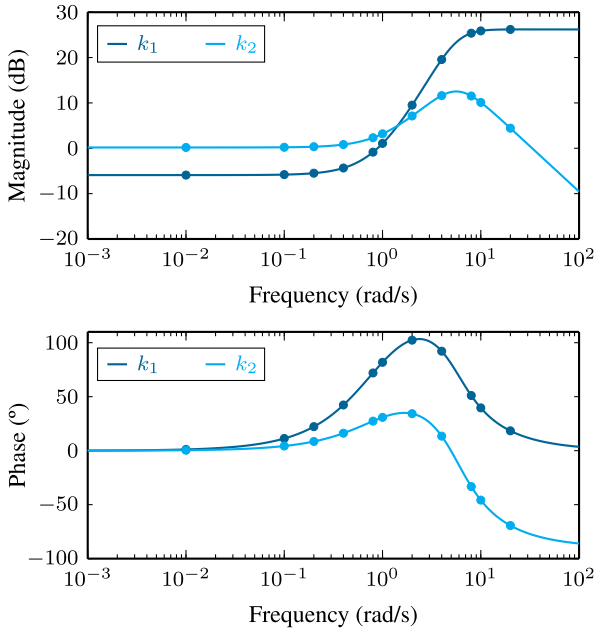

FIGURE 4. Frequency responses of $k_{1,2}$ (12).

TABLE 1. Two strategies for the frequency allocation of feedforward.

ST1. Control action reduction											
ω	0.01	0.1	0.2	0.4	0.8	1	2	4	8	10	20
p_1	×	×	×	×	×	×	×				
p_2			×	×	×	×	×	×	×	×	×
ST2. Feedback action reduction											
ω	0.01	0.1	0.2	0.4	0.8	1	2	4	8	10	20
p_1						×	×	×	×	×	
p_2	×	×	×	×	×						

action. This completes the allocation at the lower part of Table 1.

The individual feedforward elements that achieve ST1 are

$$g_1(s) = \frac{4}{s+4}, \quad g_2(s) = \frac{s}{s+0.1}. \tag{29}$$

The low-pass filter g_1 attains a cut-off frequency of $\omega_c = 4$, and the high-pass filter g_2 attains a cut-off frequency of $\omega_c = 0.1$. The individual feedforward elements that achieve ST2 are

$$g_1(s) = \frac{s}{s+1}, \quad g_2(s) = \frac{1}{(s+1)^2}. \tag{30}$$

In this case, g_1 is a high-pass filter with $\omega_c = 1$, and g_2 is a low-pass filter with $\omega_c = 0.6$. The use of individual filters g_i modifies the outcome plant p_m (10) to be handled by feedback $c_{i=1,2}$ and the remaining feedforward g_m. Fig 5 proves the objectives of both strategies: ST1 achieves a more powerful p_m plant, which will demand less $|u_i/r|$, and ST2 achieves a p_m plant with smaller uncertainty, which will require less $|u_{fb_i}/r|$.

The distribution of feedback is decided later by comparing the bounds $\beta_{c_{i=1,2}}$ in Fig 6. These bounds represent the feedback demand at each input in the event that this input handles the feedback tasks alone; SectionII-D detailed the formal procedure for computing these bounds. As expected, β_{c_i} bounds for ST2 are lower than those for ST1, for whichever

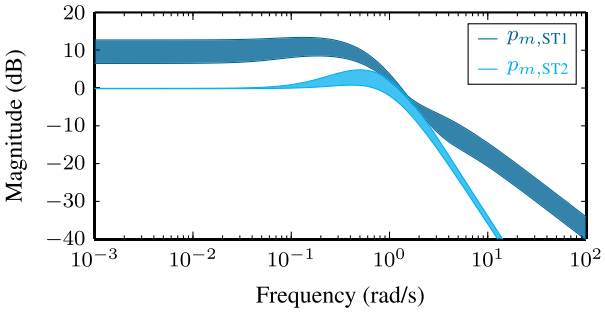

FIGURE 5. Frequency responses of the outcome plant p_m after g_i filtering.

TABLE 2. Frequency allocation of feedback for the two strategies of feedforward.

ST1. Control action reduction											
ω	0.01	0.1	0.2	0.4	0.8	1	2	4	8	10	20
p_1	×	×	×	×	×	×	×				
p_2					×	×	×	×	×	×	×
ST2. Feedback action reduction											
ω	0.01	0.1	0.2	0.4	0.8	1	2	4	8	10	20
p_1	×	×	×	×	×	×	×				
p_2					×	×	×	×	×	×	×

input assumes the control. For either of the two strategies, the feedback frequency band distribution between inputs is decided by comparing the bound heights. The results appear in Table 2, and are entirely in consonance with the plant frequency responses in Fig 3. In order to provide certain l_t, the plant p_1 is clearly more powerful than p_2 over $\omega \leq 0.4$, whereas the opposite occurs over $\omega \geq 4$. However, as the difference in magnitude between plants shortens, in particular, over $0.8 \leq \omega \leq 2$, the collaboration of both plants will help to reduce the individual feedback action.

To conduct the feedback allocation at Table 2, the design bounds β_{l_i} are computed and each $l_{i_o} = p_{i_o} c_i$ is loopshaped to meet them as Fig 7 illustrates; nominal p_{i_o} plants of (24) correspond to $a = 0.16, b = 1.36, c = 0.98, d = 1.00$. The bounds considered not only the tracking specification, but also the stability specifications. The feedback controllers for ST1 are

$$\begin{aligned} c_1(s) &= \frac{6(s+0.5)}{s(s+4)}, \\ c_2(s) &= \frac{109.01(s^2+7.219s+14.75)}{(s+15)(s^2+10.33s+39.69)}. \end{aligned} \tag{31}$$

And the feedback controllers for ST2 are

$$\begin{aligned} c_1(s) &= \frac{1.8135(s+0.013)(s+0.7)}{s(s+0.48)(s+1.5)}, \\ c_2(s) &= \frac{44.37(s+0.88)}{(s+1.7)(s+3)(s+6.6)}. \end{aligned} \tag{32}$$

Finally, the bounds on the feedforward master are computed, and the loopshaping (see Fig 8) yields the following:

$$g_m(s) = \frac{19.107(s+0.02)(s^2+0.684s+0.36)}{(s+1)(s+0.019)(s^2+6.066s+19.89)} \tag{33}$$

for ST1, and

$$g_m(s) = \frac{k(s+b_1)(s+b_2)(s^2+b_3s+b_4)}{(s+a_1)(s+a_2)(s+a_3)(s^2+a_4s+a_5)} \tag{34}$$

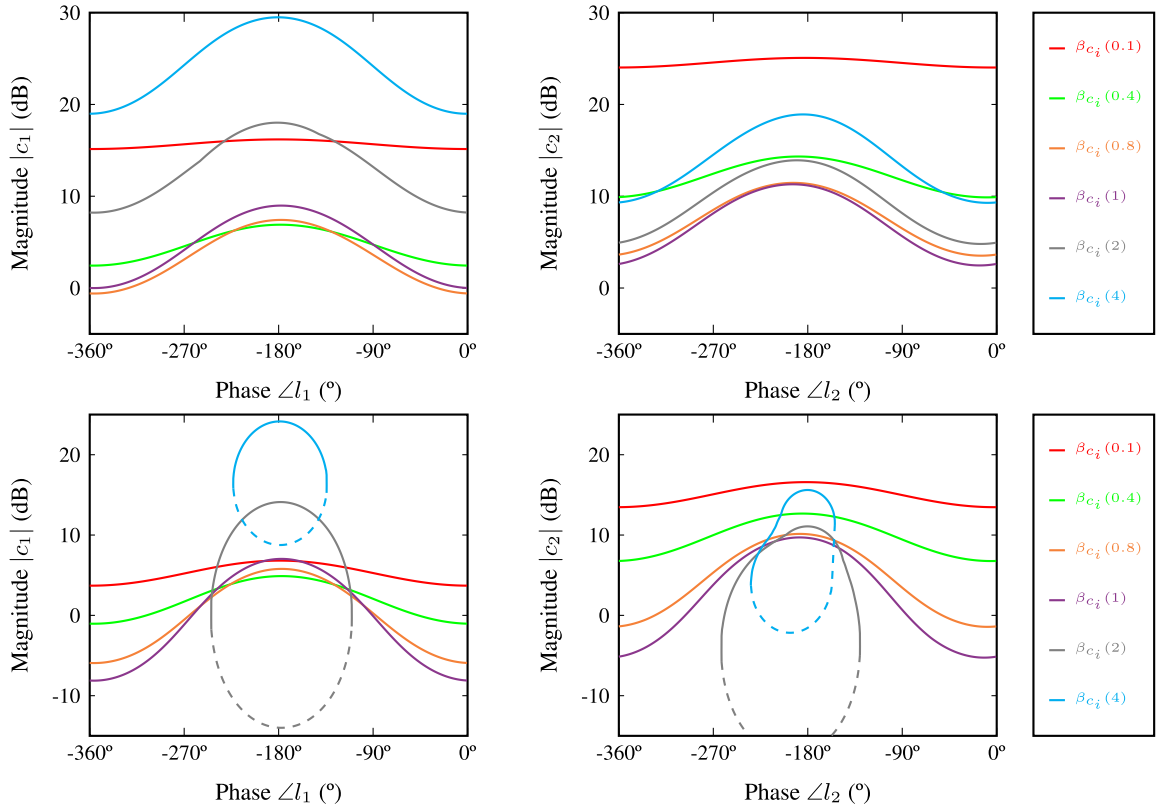

FIGURE 6. Feedback demand of (left) p_1 and (right) p_2 for strategies (up) ST1 and (down) ST2.

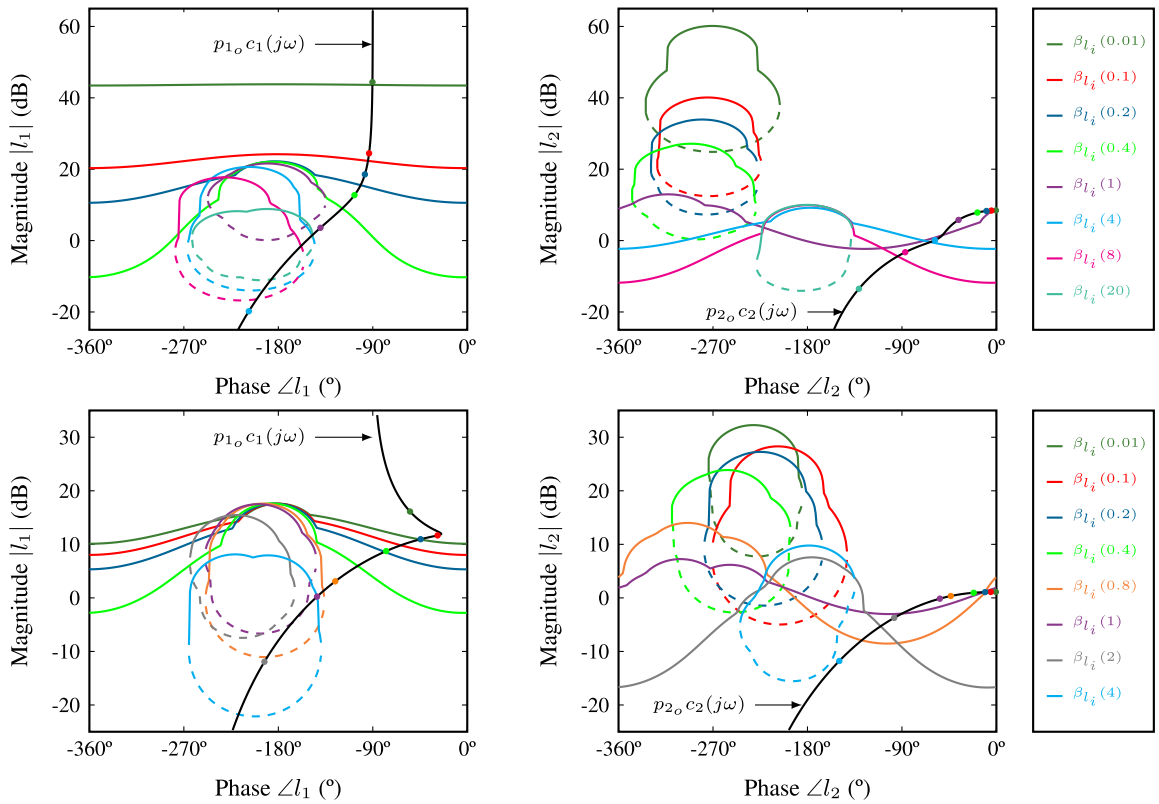

FIGURE 7. Bounds and loop-shaping for (left) c_1 and (right) c_2, and strategies (up) ST1 and (down) ST2.

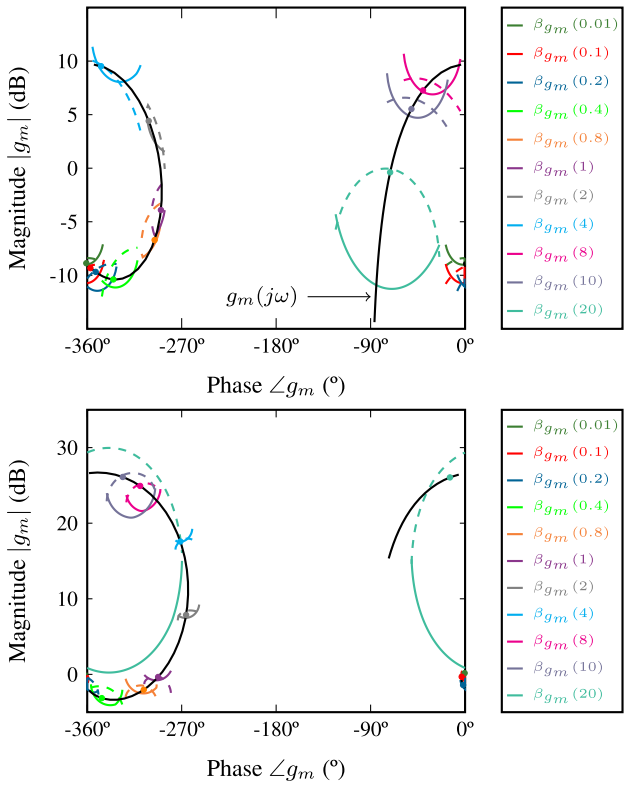

FIGURE 8. Bounds and loop-shaping of master feedforward for both strategies: (up) ST1 (down) ST2.

with coefficients of

$$\begin{aligned} k &= 597 \quad b_1 = 1.13 \quad b_2 = 10.21 \quad b_3 = 1.078 \\ b_4 &= 0.43 \quad a_1 = 0.26 \quad a_2 = 7.6 \\ a_3 &= 20 \quad a_4 = 14.9 \quad a_5 = 73.55 \end{aligned} \tag{35}$$

for ST2.

Fig 9 proves that the performance (8)(26)(27) and stability (17)(25) specifications have been fulfilled for ten plant cases in the uncertain set (24). Closely achieving performance saves control action, but requires a higher order of the control elements to exactly meet the bounds.

Fig 10 shows several analyses of interest in the frequency domain. Feedback loops $l_i = p_i c_i$ perform the feedback allocation in Table 2. Thus, $l_t \approx l_1$ over low frequencies, $l_t \approx l_2$ over high frequencies, and $l_t = l_1 + l_2$ over the mid-frequency band. ST2 shows a smaller need for feedback $|l_t(j\omega)|$ than ST1. This results in smaller $|c_{i=1,2}(j\omega)|$. All this is a consequence of the different distribution of feedforward l_g between the inputs, i.e. $l_{g_i} = p_i g_i g_m$, according to Table 1. ST2 prioritizes building a total feedforward l_g with the smallest possible uncertainty by achieving $l_g \approx l_{g_2}$ over low frequencies and $l_g \approx l_{g_1}$ over high frequencies. The main benefit of obtaining smaller $|c_{i=1,2}(j\omega)|$ is a considerably smaller amplification of v sensor noise at both u_i actuations (20). However, the price paid for using a less powerful input to provide the feedforward needed is a larger $|g_{i=1,2} g_m(j\omega)|$ at the frequencies where they participate in the control tasks. Let us compare how much larger $|g_2 g_m(j\omega)|$ of ST2 is than $|g_1 g_m(j\omega)|$ of ST1 over low frequencies. In contrast, $|g_1 g_m(j\omega)|$ of ST2 is much larger than $|g_2 g_m(j\omega)|$ of ST1 over high frequencies. Time domain responses in Fig 11 clearly show these drawbacks; the system is excited with a unit step $r(t)$ at $t = 1$. ST2 demands smaller $u_{fb_i}(t)$ than ST1. However, its relevance in $u_i(t)$ is far less than $u_{ff_i}(t)$. Eventually, ST1 uses less $u_i(t)$ at both inputs. In particular, ST2 requires a larger actuation range for u_1 during the transients, and implies larger expends of u_2 at steady state. A fair comparison would compare the steady state of u_1 in ST1 with the steady state of u_2 in ST2, as these are the inputs that provide the actuation to achieve $r = y$ in steady state. Even for this comparison, ST1 achieves better results than ST2.

As expected in MISO control, the inputs that do not work at steady state (u_2 for ST1 and u_1 for ST2) return to zero at $t = \infty$, i.e., they recover a convenient chosen operating point r_{u_i}. Section II-E detailed the requirements to provide this and to achieve $r = y$ at $t = \infty$, named as follows. In ST1, an integrator is needed in c_1 (31) and a differentiator in g_2 (29). In ST2, an integrator is needed in c_1 (32) and a differentiator in g_1 (30).

B. EXAMPLE 2

This second example shows the benefits of the new structure that conveniently adds feedforwad loops and highlights the relevance of a robust design method.

As a reference, let us take the solution given by ST1 of Example 1, which yielded feedback controllers (31) and feedforward elements (29) (33) to govern the two-input system (24) inside the control structure of Fig 2, being $n = 2$.

This is being compared with one of the most popular multi-input control strategies in process industry: *valve position control* (VPC) [14], [26]. Its quick and effective design method is oriented to simple process models without uncertainty. Thus, let us take the nominal plants

$$p_{1_o}(s) = \frac{2}{(s+0.7)^2}, \quad p_{2_o}(s) = \frac{2}{s+2}, \tag{36}$$

from the uncertain set (24) for a fairer comparison (their magnitude frequency responses are centred on the bunch of p_1 and p_2 responses, respectively, on Fig 3). VPC employs a serial structure of feedback controllers - Fig 12- and the following design method [26].

A PI controller $c_2(s)$ to the fastest input (p_{2_o} plant) is first designed to achieve the desired y/r performance, i.e m (26). To accomplish the design, [26] suggests any standard procedure. Here,

$$c_2(s) = 3\left(1 + \frac{1}{0.1837s}\right), \tag{37}$$

is found to place the roots of $1 + p_{2_o} c_2(s)$ at the poles of m. After the quick response of the fastest loop $l_2 = p_{2_o} c_2$, the slowest loop $l_1 = p_{1_o} c_1 c_2$ must take charge of the system, and the fastest input u_2 must be reset to a convenient set-point r_{u_2} (*mid-ranging*). Thus, another PI controller $c_1(s)$ determines the switching frequency ω_{sw} between loops,

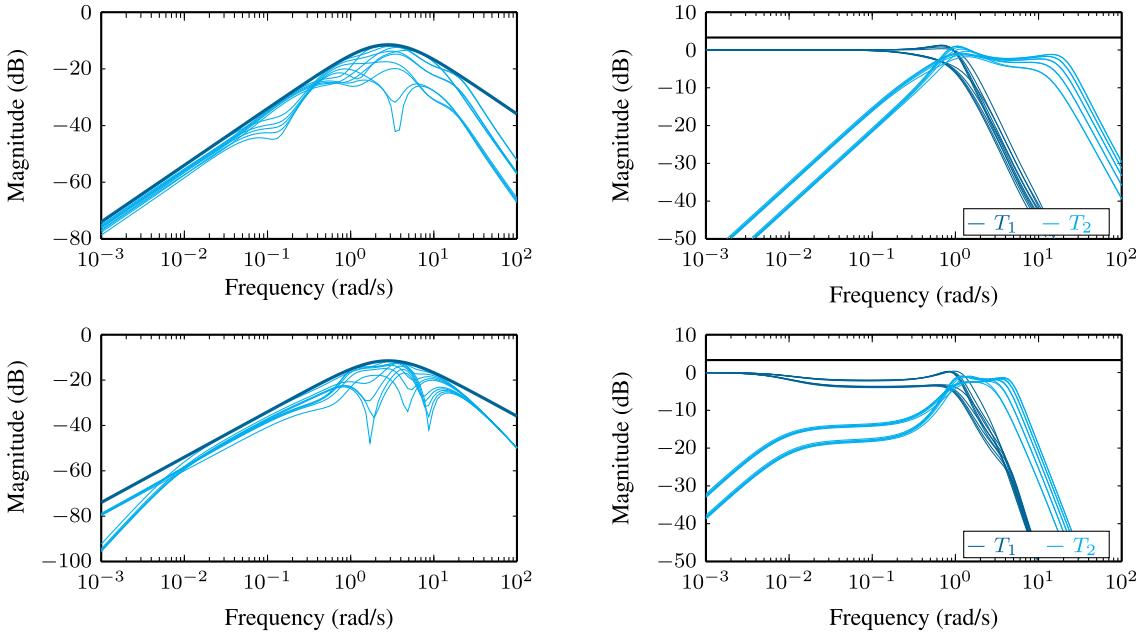

FIGURE 9. Robust (left) tracking error and (right) stability, for strategies (up) ST1 (down) ST2.

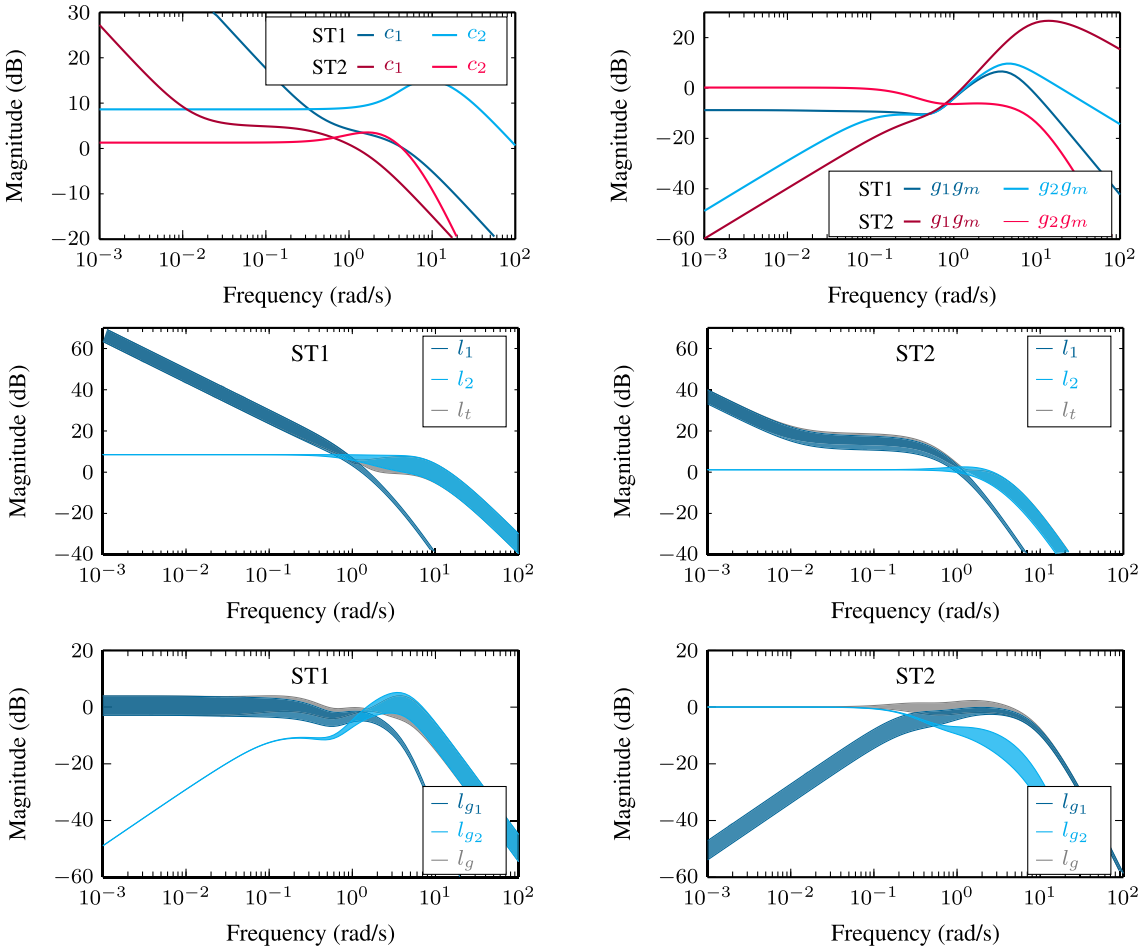

FIGURE 10. Magnitude frequency responses of control elements and loop functions.

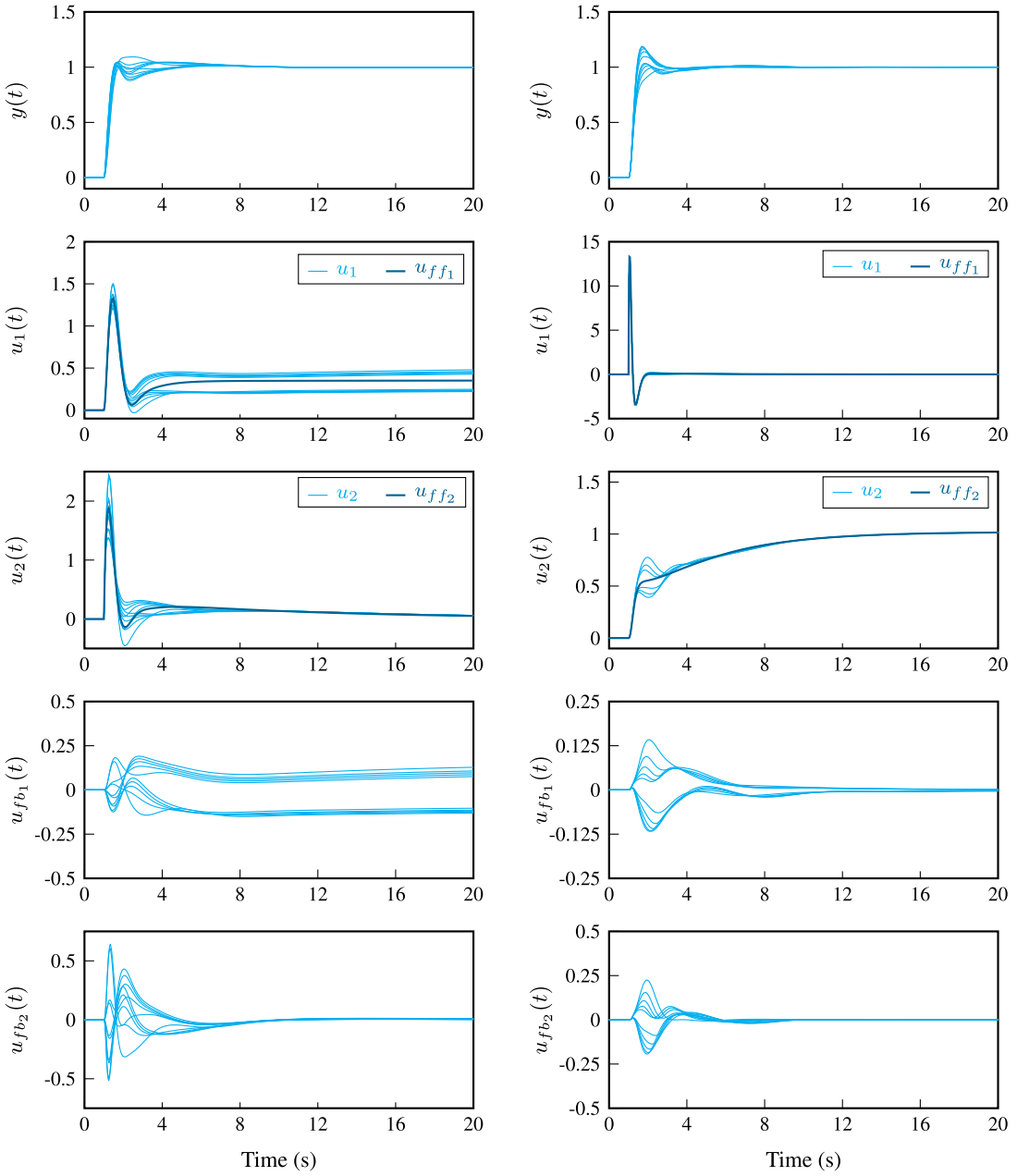

FIGURE 11. Time domain responses of output and control inputs for (left) ST1 (right) ST2.

where $|l_1(j\omega_{sw})| = |l_2(j\omega_{sw})|$. There is not a standard method to choose ω_{sw}, but it must be sufficiently lower than the fast loop crossover frequency ω_{c_2} to avoid any distortion of the performance m already achieved. This impedes any collaboration of plants as ST1 reached over $\omega \in [0.8, 2]$ (see Table 2), i.e. VPC forces plants to work in separated frequency bands. To get a behaviour comparable to ST1, $\omega_{sw} = 0.4$ is selected. Then, the PI time integral is tuned to $\omega_{sw}/5$ as [26] recommends. Finally, the PI proportional gain is calculated to achieve $|l_1(j\omega_{sw})| = |l_2(j\omega_{sw})|$. The VPC controller is

$$c_1(s) = 12.5\left(1 + \frac{1}{0.0843s}\right). \tag{38}$$

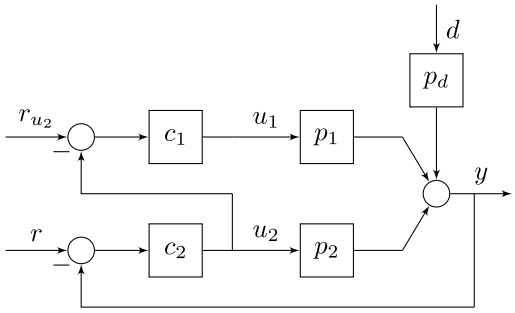

FIGURE 12. Series architecture in *valve position control*.

Fig 13 compares the robust feedback plus feedforward of the new QFT strategy with the feedback-only of VPC.

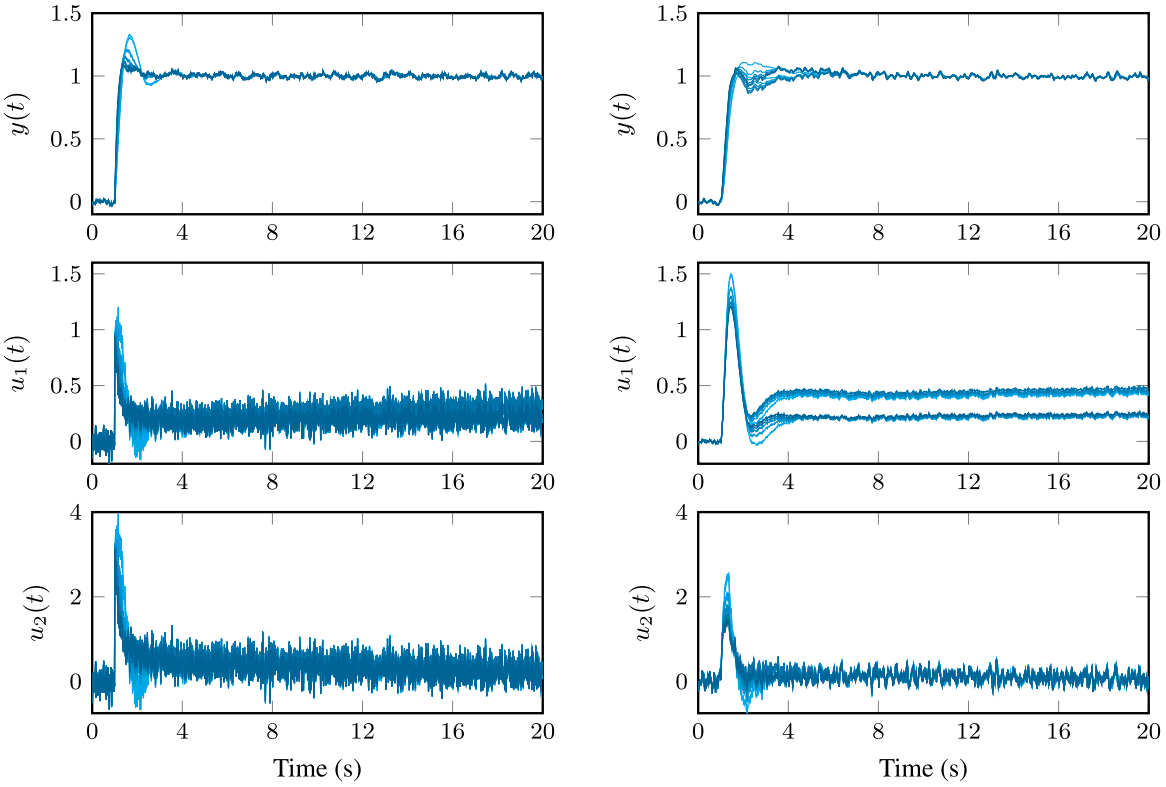

FIGURE 13. Time domain responses of output and control inputs for (left) feedback VPC (right) feedback-feedforward QFT.

External inputs are a unit step change of set-point $r(t)$ at $t = 1$ s and a sensor noise $v(t)$ that is built with a band limited white-noise source of Simulink®(power of 0.00005 and sample time of 0.01 s).

Both strategies show a similar behaviour $y(t)$. Nevertheless, VPC presents a three times higher overshoot due to the c_2 zero (37) that is transmitted to y/r transfer function and distorts the pure second order behaviour of m. Despite any fine tuning of feedback c_2 to palliate the overshoot for the nominal case, this does not guarantee a proper behaviour for another plant case, since VPC is not a robust method and does not consider the plant uncertainty in the design. Another solution would be to incorporate a feedforward prefilter to the classical feedback structure, as it is common in SISO control. Our methodology illustrates the more profitable way of adding feedforward elements to MISO control and achieves the expected performance for the whole set of plant cases.

Nevertheless, the major differences are on control actions $u_1(t)$ and $u_2(t)$. Our parallel structure of feedback controllers allows a free and flexible allocation of the frequency band between inputs [19]. The plant collaboration over mid-frequencies ($\omega \in [0.8, 2]$) increases the $u_1(t)$ peak to help the fast intervention of $u_2(t)$. Then, a more balanced pair of u_1 and u_2 peaks than in VPC is obtained; it should be recalled that both loops work on clearly separated frequency bands in VPC. The benefit of collaboration to reduce the control action would be even more advantageous the higher the gain of the plants in the same frequency band.

Another drawback of $\omega_{sw} \ll \omega_{c_2}$ in VPC is a slower return of $u_2(t)$ to the set-point $r_{u_2}(t)$, which is supposed to be a profitable steady state [2], [14]–[18]. In particular, $u_2(t)$ shows a settling time three times longer for feedback-only VPC than for feedback-feedforward QFT. Those effects would be even more noticeable with traditional VPC strategies [14], which seek slower $u_1(t)$ intervention.

Finally, the most relevant difference is the amplification of the sensor noise $v(t)$ at the control inputs $u_{i=1,2}(t)$, which is favoured by the feedback control gains $|c_{i=1,2}(j\omega)|$. From a mathematical point of view, (8) shows how a non-zero $\sum_{i=1}^{n} p_i g_i g_m$ can help to reduce the c_i feedback gains, as in SISO control, and this happens regardless of the design technique. In the present example, compare the $c_2(j\omega)$ gain (31) with (37), and also the $c_1(j\omega)$ gain (31) with the $c_1c_2(j\omega)$ gain (38)(37) that results from the equivalent of a series structure to a parallel one. Ultimately, too much noise at the control inputs causes fatigue or even saturation of the actuators. Let us quantify the differences between both strategies by computing the indices

$$IAVU_{i=1,2} = \int_0^t \left| \frac{du_i(\tau)}{d\tau} \right| dt \tag{39}$$

for the ten plant cases. Table 3 shows the results. The feedback-only strategy returns an index 15.3 times higher for u_1 and 3.94 times higher for u_2 than the feedback-feedforward strategy, showing the superiority of the latter.

TABLE 3. Noise effect at the control inputs (39).

	Feedback VPC	Feedback-feedforward QFT
$IAVU_1$	[1.4256, 1.4659]	[0.0868, 0.0931]
$IAVU_2$	[4.7538, 4.8883]	[1.2074, 1.2218]

C. REMARKS

- When several control inputs are available, a convenient distribution of the control bandwidth can help to reduce the individual control action in addition to satisfying the performance specification for the output. A method is established that relates the plant frequency responses to the performance specification.
- Feedforward from known external inputs reduces the feedback contribution and its drawbacks, namely the amplification of sensor noise at the control inputs, which can saturate or fatigue actuators.
- The presented control architecture allows an independent distribution of frequencies for feedback and feedforward tasks. Thus, plants can collaborate or be inhibited at any design frequency, for feedback or feedforward.
- As a preference, the frequency distribution of feedforward aims to use the least possible control action at each input, but any other strategy is supported. For example, feedforward can be oriented to use the least possible feedback action despite increasing the total control effort. This strategy could be of interest for systems with a high level of sensor noise.
- The control structure supports any number of control inputs, and the method can handle any plant difficulties such as pure delays or RHP zeros and poles.
- A robust methodology guarantees the expected benefits for a predefined set of plant cases. Robust model matching for reference tracking and robust stability were explicitly considered. Other robust specifications such as disturbance rejection and set-point changes for the mid-range variables could also be added.

IV. CONCLUSION

Several control inputs contributed to output performance by allocating their participation along the control bandwidth, which resulted in the use of the least possible control action. This demand ultimately depended on the input-output (plant) frequency response and the required performance. Due to uncertainties about plant models and unknown disturbances, the usual means to compute the control actions were inside feedback loops. If some external inputs were accessible (output reference), feedforward helped feedback to generate the required action. This reduced, in single-input control, the amount of feedback and its high frequency drawbacks. However, using the feedforward to minimise the feedback might prove to be faulty in multi-input control. Since there were several available inputs, a thoughtful feedforward and feedback distribution attempted to minimise the control action at each input, which reported benefits at all frequencies. The expected results were: (i) lower expenses in the inputs that handle the steady state, (ii) greater ranges of actuation in the inputs that handle the transients, and (iii) less noisy commands on actuators.

The proposed control architecture contained feedback loops (one feedback controller in the direct path to each control input) and incorporated feedforward loops straight to the control inputs (a master feedforward followed by individual pass-band filters). This enabled a tailor-made and separated distribution of feedback and feedforward, which improved classical mid-ranging control that used feedback-only architectures and clearly separated frequency bands for each input intervention. In the new method, first, individual feedforward filters allocated the control bandwidth so that an equivalent plant was built with equal or greater magnitude at each frequency than any individual plant. Next the uncertainty of this equivalent plant was addressed. Thus, global feedback reduced the closed loop deviation of magnitude frequency responses to the extent that, at a second step, a master feedforward could place them in-between the tolerances of model-matching. Individual feedback controllers distributed the global feedback among the inputs. In so doing, they sought to use the least possible feedback at each frequency. Quantitative Feedback Theory (QFT) was the robust methodology used to design the control elements, which achieved the expected benefits for the whole set of plant cases. In QFT framework, a new formulation was developed to deal with more general robust control specifications.

In future work, the feedforward of any other measurable input, such as measurable disturbances, may be of interest, which will need a specific analysis. Additionally, we intend to take advantage of the new control structures in an application example.

APPENDIX I
INEQUALITY FOR CAD COMPUTATION OF FEEDBACK CONTROLLER BOUNDS

A general format of robust control specification with feedback G and feedforward G_f elements is the following:

$$\left|\frac{AG_f + B}{C + DG}\right| \leq W, \tag{40}$$

where A, B, C and D are known functions that can take a set of values (uncertainty), and W is the upper tolerance of the magnitude of the closed-loop frequency response.

QFT perspective limits the feedback to the strictly necessary amount that enables a feedforward controller to be found. Thus, the method begins to find the mathematical requirements over G. Equation (40) is rearranged as

$$\left|G_f + \frac{B}{A}\right| \leq W\frac{|C + DG|}{|A|}. \tag{41}$$

Then, considering G_f as the independent variable, (41) describes the region of valid feedforward elements G_f in the complex plane for each frequency of interest. This region is a circle with centre $-B/A$ and radius $W|C + DG|/|A|$. Thus, any two cases (u, v) of A, B, C and D in the set of possible values share a common solution G_f if the distance between

the centres of the circles is equal to, or shorter than, the sum of their radii. This condition is expressed by the inequality below:

$$\left|\frac{B_u}{A_u}-\frac{B_v}{A_v}\right| \le W\frac{|C+D_uG|}{|A_u|}+W\frac{|C_v+D_vG|}{|A_v|}. \quad (42)$$

This expresses the requirements of G. It is conveniently rearranged as

$$|B_uA_v-B_vA_u| \le W|C+D_uG||A_v|+W|C_v+D_vG||A_u|. \quad (43)$$

All of the frequency responses can be written in polar form as $A=a\angle\theta_a$, $B=b\angle\theta_b$, $C=c\angle\theta_c$, $d=d\angle\theta_d$, $G=g\angle\phi$. Thus, the modulus of sum vectors in (43) can be expanded using Euler's formula as

$$\begin{aligned}|B_uA_v-B_vA_u| &= \big(b_u^2a_v^2+b_v^2a_u^2-2b_ub_va_ua_v \\ &\quad\times\cos(\theta_{b,u}+\theta_{a,v}-\theta_{b,v}-\theta_{a,u})\big)^{1/2}, \quad (44)\\ |C_v+D_vG| &= \big(d_v^2g^2+c_v^2+2c_vd_vg\cos(\psi_v)\big)^{1/2}, \quad (45)\\ |C_u+D_uG| &= \big(d_u^2g^2+c_u^2+2c_ud_ug\cos(\psi_u)\big)^{1/2}; \quad (46)\end{aligned}$$

where

$$\begin{aligned}\psi_v &= \phi+\theta_{d,v}-\theta_{c,v},\\ \psi_u &= \phi+\theta_{d,u}-\theta_{c,u}.\end{aligned} \quad (47)$$

And inserting them into (43) yields

$$\begin{aligned}&\big(b_u^2a_v^2+b_v^2a_u^2-2b_ub_va_ua_v\cos(\theta_{b,u}+\theta_{a,v}-\theta_{b,v}-\theta_{a,u})\big)^{1/2}\\ &\le Wa_v\big(d_u^2g^2+c_u^2+2c_ud_ug\cos(\psi_u)\big)^{1/2}\\ &\quad+Wa_u\big(d_v^2g^2+c_v^2+2c_vd_vg\cos(\psi_v)\big)^{1/2}. \quad (48)\end{aligned}$$

After squaring both sides of the inequality twice and rearranging, a fourth order inequality on g is produced:

$$\lambda_4g^4+\lambda_3g^3+\lambda_2g^2+\lambda_1g+\lambda_0 \le 0 \quad (49)$$

where

$$\begin{aligned}\lambda_4 &= \frac{-(a_v^2d_u^2-a_u^2d_v^2)^2}{4a_v^2a_u^2}\\ \lambda_3 &= d_vc_v\cos(\psi_v)(d_u^2-\frac{a_u^2}{a_v^2}d_v^2)\\ &\quad+d_uc_u\cos(\psi_u)(d_v^2-\frac{a_v^2}{a_u^2}d_u^2)\\ \lambda_2 &= d_u^2c_v^2+c_u^2d_v^2+\widehat{W}\left(\frac{a_v}{a_u}d_u^2+\frac{a_u}{a_v}d_v^2\right)\\ &\quad-\left(\frac{a_v}{a_u}c_ud_u\cos(\psi_u)-\frac{a_u}{a_v}c_vd_v\cos(\psi_v)\right)^2\Big]\\ \lambda_1 &= 2c_vd_v(c_u^2+\frac{a_u}{a_v}\widehat{W})\cos(\psi_v)\\ &\quad+2c_ud_u(c_v^2+\frac{a_v}{a_u}\widehat{W})\cos(\psi_u)\\ \lambda_0 &= c_u^2c_v^2-\widehat{W}^2\end{aligned} \quad (50)$$

and

$$\begin{aligned}\widehat{W} &= \frac{a_v}{a_u}\left(\frac{b_u^2-c_u^2W^2}{2W^2}\right)+\frac{a_u}{a_v}\left(\frac{b_v^2-c_v^2W^2}{2W^2}\right)\\ &\quad-\frac{b_ub_v}{W^2}\cos(\theta_{b,u}+\theta_{a,v}-\theta_{b,v}-\theta_{a,u}).\end{aligned} \quad (51)$$

The squaring operations introduced non-valid solutions. Thus, the four g solutions of (49) must be checked and, those that do not fulfil (43) must be discarded. As is common in QFT, the procedure is repeated for all possible pairs (u, v) in the uncertain set. Finally, a controller bound can be calculated at ω. This delimits the valid region for g at each phase ϕ on the mod-arg plane.

Controller bounds are calculated for a discrete set of frequencies and then referred to a nominal plant P_o to perform the loopshaping $L_o = P_oG$ on a mod-arg plot. Thus, the bound solution $G = g\angle\phi$ is shifted by $P_o = p_o\angle\theta_o$. The nominal plant corresponds to the nominal case of the uncertain set of A, B, C, D. In this way, (49) can be easily incorporated in the Terasoft QFT toolbox [23], which to date has used quadratic inequalities on g to calculate bounds for different closed-loop inequalities (see functions *sisobnds* and *gndbnds*).

Also, it can be proven that the controller solution (49) to meet the robust specification (43) is simplified in the controller solution given in [22] to solve $\left|(M-PG_f)/(1+PG)\right| \le W$. Let us use the following equivalents $A=-P$, $B=M$, $C=1$, $D=P$, and their polar forms $a\angle\theta_a = p\angle-\theta$, $b\angle\theta_b = m\angle\mu$, $c\angle\theta_c = 1\angle0$, $d\angle\theta_d = p\angle\theta$. After substituting their particular values (u, v) in (50), the following is obtained:

$$\begin{aligned}\lambda_4 &= \frac{(p_v^2p_u^2-p_u^2p_v^2)^2}{4p_v^2p_u^2}\\ \lambda_3 &= p_v\cos(\phi+\theta_v)(p_u^2-\frac{p_u^2}{p_v^2}p_v^2)\\ &\quad+p_u\cos(\phi+\theta_u)(p_v^2-\frac{p_v^2}{p_u^2}p_u^2)\\ \lambda_2 &= p_u^2+p_v^2+\widehat{W}\left(\frac{p_v}{p_u}d_u^2+\frac{p_u}{p_v}p_v^2\right)\\ &\quad-\left(\frac{p_v}{p_u}p_u\cos(\phi+\theta_u)-\frac{p_u}{p_v}p_v\cos(\phi+\theta_v)\right)^2\\ \lambda_1 &= 2p_v(1+\frac{p_u}{p_v}\widehat{W})\cos(\phi+\theta_v)\\ &\quad+2p_u(1+\frac{p_v}{p_u}\widehat{W})\cos(\phi+\theta_u)\\ \lambda_0 &= 1-\widehat{W}^2,\end{aligned} \quad (52)$$

where

$$\begin{aligned}\widehat{W} &= \frac{p_v}{p_u}\left(\frac{m_u^2-W^2}{2W^2}\right)+\frac{p_u}{p_v}\left(\frac{m_v^2-W^2}{2W^2}\right)\\ &\quad-\frac{m_um_v}{W^2}\cos(\mu_u-\theta_v-\mu_v+\theta_u).\end{aligned} \quad (53)$$

Since the performance model M has no uncertainty ($m_u = m_v = m$ and $\mu_u = \mu_v = \mu$),

$\widehat{W}$ can be rewritten as

$$\widehat{W} = \frac{p_v}{p_u}\left(\frac{m^2 - W^2}{2W^2}\right) + \frac{p_u}{p_v}\left(\frac{m^2 - W^2}{2W^2}\right) - \frac{m^2}{W^2}\cos(\theta_u - \theta_v). \quad (54)$$

By means of simple operations, one can verify how the coefficients λ_4 and λ_3 vanish and (49) simplifies to

$$g^2\left(p_u^2 + p_v^2 + 2p_u p_v \widehat{W} - (p_v\cos(\phi+\theta_u) - p_u\cos(\phi+\theta_v))^2\right) + 2g\left((p_v + p_u\widehat{W})\cos(\phi+\theta_v) + (p_u + p_v\widehat{W})\cos(\phi+\theta_u)\right) + (1-\widehat{W}^2) \le 0, \quad (55)$$

which matches the quadratic inequality in [22].

REFERENCES

[1] O. Johnsson, D. Sahlin, J. Linde, G. Lidén, and T. Hägglund, "A mid-ranging control strategy for non-stationary processes and its application to dissolved oxygen control in a bioprocess," *Control Eng. Pract.*, vol. 42, pp. 89–94, Sep. 2015.

[2] S. Nájera, M. Gil-Martínez, and J. Rico-Azagra, "Dual-control of autothermal thermophilic aerobic digestion using aeration and solid retention time," *Water*, vol. 9, no. 6, p. 426, Jun. 2017.

[3] P. A. Luppi, L. Braccia, P. G. Rullo, and D. A. R. Zumoffen, "Plantwide control design based on the control allocation approach," *Ind. Eng. Chem. Res.*, vol. 57, no. 1, pp. 268–282, Jan. 2018.

[4] K. van Heusden, J. M. Ansermino, and G. A. Dumont, "Robust MISO control of propofol-remifentanil anesthesia guided by the NeuroSENSE monitor," *IEEE Trans. Control Syst. Technol.*, vol. 26, no. 5, pp. 1758–1770, Sep. 2018.

[5] H. Li, C. Du, and Y. Wang, "Optimal reset control for a dual-stage actuator system in HDDs," *IEEE/ASME Trans. Mechatronics*, vol. 16, no. 3, pp. 480–488, Jun. 2011.

[6] J. Zheng and M. Fu, "A unified dual-stage actuator control scheme for track seeking and following in hard disk drives," *IET Control Theory Appl.*, vol. 6, no. 10, pp. 1468–1477, Jul. 2012.

[7] Z. Ma, A.-N. Poo, M. H. Ang, G.-S. Hong, and H.-H. See, "Design and control of an end-effector for industrial finishing applications," *Robot. Comput.-Integr. Manuf.*, vol. 53, pp. 240–253, Oct. 2018.

[8] C. Nainer, M. Furci, A. Seuret, L. Zaccarian, and A. Franchi, "Hierarchical control of the over-actuated ROSPO platform via static input allocation," *IFAC-PapersOnLine*, vol. 50, no. 1, pp. 12698–12703, 2017.

[9] U. Schneider, B. Olofsson, O. Sörnmo, M. Drust, A. Robertsson, M. Hägele, and R. Johansson, "Integrated approach to robotic machining with macro/micro-actuation," *Robot. Comput.-Integr. Manuf.*, vol. 30, no. 6, pp. 636–647, Dec. 2014.

[10] T. Haus, A. Ivanovic, M. Car, M. Orsag, and S. Bogdan, "Mid-ranging control concept for a multirotor UAV with moving masses," in *Proc. 26th Medit. Conf. Control Autom. (MED)*, Jun. 2018, pp. 339–344.

[11] S. Jade, J. Larimore, E. Hellstrom, L. Jiang, and A. G. Stefanopoulou, "Enabling large load transitions on multicylinder recompression HCCI engines using fuel governors," in *Proc. Amer. Control Conf.*, Jun. 2013, pp. 4423–4428.

[12] T. A. Johansen and T. I. Fossen, "Control allocation—A survey," *Automatica*, vol. 49, no. 5, pp. 1087–1103, May 2013.

[13] M. Cocetti, A. Serrani, and L. Zaccarian, "Linear output regulation with dynamic optimization for uncertain linear over-actuated systems," *Automatica*, vol. 97, pp. 214–225, Nov. 2018.

[14] B. J. Allison and S. Ogawa, "Design and tuning of valve position controllers with industrial applications," *Trans. Inst. Meas. Control*, vol. 25, no. 1, pp. 3–16, Mar. 2003.

[15] M. A. Henson, B. A. Ogunnaike, and J. S. Schwaber, "Habituating control strategies for process control," *AIChE J.*, vol. 41, no. 3, pp. 604–618, Mar. 1995.

[16] B. J. Allison and A. J. Isaksson, "Design and performance of mid-ranging controllers," *J. Process Control*, vol. 8, nos. 5–6, pp. 469–474, Oct. 1998.

[17] W. L. Luyben, *Chemical Reactor Design and Control*. Hoboken, NJ, USA: Wiley, 2007.

[18] M. Gil-Martínez, J. Rico-Azagra, and J. Elso, "Frequency domain design of a series structure of robust controllers for multi-input single-output systems," *Math. Problems Eng.*, vol. 2018, pp. 1–14, Oct. 2018.

[19] J. Rico-Azagra, M. Gil-Martínez, and J. Elso, "Quantitative feedback control of multiple input single output systems," *Math. Problems Eng.*, vol. 2014, pp. 1–17, Apr. 2014.

[20] M. Gil-Martínez and J. Rico-Azagra, "Robust feedback control for non-minimum phase, delayed, or unstable systems with multiple inputs," *Math. Problems Eng.*, vol. 2020, pp. 1–18, Apr. 2020.

[21] I. Horowitz, "Survey of quantitative feedback theory (QFT)," *Int. J. Robust Nonlinear Control*, vol. 11, no. 10, pp. 887–921, 2001.

[22] J. Elso, M. Gil-Martínez, and M. García-Sanz, "Quantitative feedback–feedforward control for model matching and disturbance rejection," *IET Control Theory Appl.*, vol. 7, no. 6, pp. 894–900, Apr. 2013.

[23] C. Borghesani, Y. Chait, and O. Yaniv, *Quantitative Feedback Theory Toolbox. For Use With MATLAB*, 2nd ed. San Diego, CA, USA: Terasoft, 2002.

[24] J. Elso, M. Gil-Martinez, and M. Garcia-Sanz, "Quantitative feedback control for multivariable model matching and disturbance rejection," *Int. J. Robust Nonlinear Control*, vol. 27, no. 1, pp. 121–134, 2017.

[25] J. Rico-Azagra, M. Gil-Martínez, R. Rico, and P. Maisterra, "QFT bounds for robust stability specifications defined on the open-loop function," *Int. J. Robust Nonlinear Control*, vol. 28, no. 3, pp. 1116–1125, Feb. 2018.

[26] T. Hägglund, "A feedforward approach to mid-ranging control," *Control Eng. Pract.*, vol. 108, Mar. 2021, Art. no. 104713.

JAVIER RICO-AZAGRA received the master's degree in industrial engineering and the Ph.D. degree from the University of La Rioja, Spain, in 2009 and 2017, respectively. He is currently an Assistant Professor of systems engineering and automation at the University of La Rioja. He has published several articles in reputed journals in the field of robust control theory (quantitative feedback theory). He is currently leading research projects and participating in publications on unmanned aerial systems. He is a member of the Spanish Association of Automatic Control (CEA).

MONTSERRAT GIL-MARTÍNEZ received the master's degree in electrical and control engineering from the University of Cantabria, Spain, in 1995, and the Ph.D. degree in industrial engineering from the Public University of Navarra, Spain, in 2001. She is currently an Associate Professor of systems engineering and automation and the Leader of the Control Engineering Research Group, University of La Rioja, Spain. She has published several articles in reputed journals in the fields of robust control theory (quantitative feedback theory) and in control applied to waste-water treatments. She is currently participating in research projects and publications on unmanned aerial systems. She is a member of the Spanish Association of Automatic Control (CEA).